Available online at www.sciencedirect.com
ScienceDirect
Journal of Sound and Vibration 311 (2008) 756–766
JOURNAL OF SOUND AND VIBRATION
www.elsevier.com/locate/jsvi

Vibration control of shadow-mask with tension gradient using multiple dynamic absorber

Won-Jin Kim*, Chong-Hyun Park

School of Mechanical and Automotive Engineering, Keimyung University, 1000, Shindang-dong, Dalseo-gu, Taegu 704-701, Republic of Korea

Received 11 August 2006; received in revised form 21 June 2007; accepted 24 September 2007
Available online 19 November 2007

Abstract

Damping wires have been used to reduce the vibration of the shadow-mask of a large-size cathode-ray-tube (CRT). However, because the wires are very thin and are equipped on the surface of the shadow-mask, they have some limitations. Specifically, difficulty in their construction is typically encountered and they create a shadow on the screen of the CRT when applied to the shadow-mask. In this work, a multiple dynamic absorber (MDA) is introduced to effectively reduce vibration of the shadow-mask and circumvents the aforementioned limitations. The design method of the MDA is developed based on the theory of a simple dynamic absorber, because the shadow-mask has well separated and locally deformed vibration modes. The design of the dynamic absorber should involve the specification of three parameters: mass, damping ratio, and tuning frequency. In order to determine the design criteria of the MDA, a sensitivity analysis of these three parameters is executed using a finite element (FE) model of the shadow-mask. The MDA designed via the proposed method is applied to the shadow-mask and tested numerically and experimentally in order to assess its vibration reduction efficiency.

1. Introduction

A cathode-ray-tube (CRT), which is generally used for computer monitors and TV sets, is composed of a glass envelope and inner components. Among its parts, a shadow-mask plays an important role in selecting red, green, and blue (RGB) to display the picture on the screen. However, the shadow-mask is inevitably excited by vibration of built-in speakers or unexpected impact on the outer surface of the CRT.

Recently, a tension-type shadow-mask, which has a V-shaped tension distribution [1], has become the preferred option for large-sized TV sets, because it makes only a local vibration of the shadow-mask at a specific excitation frequency. However, since the shadow-mask is equipped in vacuum without air damping, it still suffers from a serious vibration problem. Very thin wires known as damping wires have also been used to reduce the vibration of the shadow-mask. They exert damping effects realized by collision and friction between the damping wires and the shadow-mask [2–4]. While this method can effectively reduce the vibration, it entails some disadvantages such as difficulty in construction of the thin wires and the appearance of shadow lines on the screen.

*Corresponding author. Tel.: +82 53 580 5265; fax: +82 53 580 5165.
E-mail address: wjkim@kmu.ac.kr (W.-J. Kim).

0022-460X/$ - see front matter © 2007 Elsevier Ltd. All rights reserved.
doi:10.1016/j.jsv.2007.09.043

In this work, a multiple dynamic absorber (MDA), which consists of several cantilevers with a thin-plate shape, is employed to overcome these limitations. A sensitivity analysis of design parameters is performed using a finite element (FE) model of the shadow-mask, yielding useful design criteria of the MDA. The proposed method is based on the theory of a simple dynamic absorber [5–8]. The advantages of the proposed approach are: (1) it effectively reduces vibration of the shadow-mask relative to the vibration reduction achieved by the damping wire; (2) it is easy to construct; and (3) it does not create a shadow on the screen because it is equipped at the edge of the shadow-mask.

2. Modal analysis of the shadow-mask

The modal analysis of the primary system provides significant information about the tuning frequencies, placement positions, and dimensions of the dynamic absorbers. A modal analysis of the shadow-mask is therefore performed using the FE method. If we assume that the shadow-mask, which is a steel thin plate with an array of many holes, is an anisotropic plate, then its material properties can be calculated on the basis of the equivalent method [9,10]. In order to consider the tension distribution of the shadow-mask, a tension analysis is executed prior to the modal analysis. The tension of the shadow-mask can be approximated in terms of a cosine function

$$T(x) = \frac{T_t - T_b}{2} \cos \frac{2\pi}{L} x + \frac{T_t + T_b}{2} \quad (0 \leqslant x \leqslant L), \tag{1}$$

where L is the width of the shadow-mask and x is an arbitrary position. T_t and T_b denote the maximum and minimum values of tension, respectively. The FE model with tension variation in the longitudinal direction is shown in Fig. 1. Fig. 2 shows four main natural frequencies and mode shapes obtained from the modal analysis. The mode shapes have local deformations with a narrow band, and maximum deformations at different positions.

3. Multiple dynamic absorber design

As previously noted, each vibration mode has a local deformation shape in a specific area. Therefore, the proposed MDA utilizes several dynamic absorbers corresponding to the vibration modes. Fig. 3 shows the

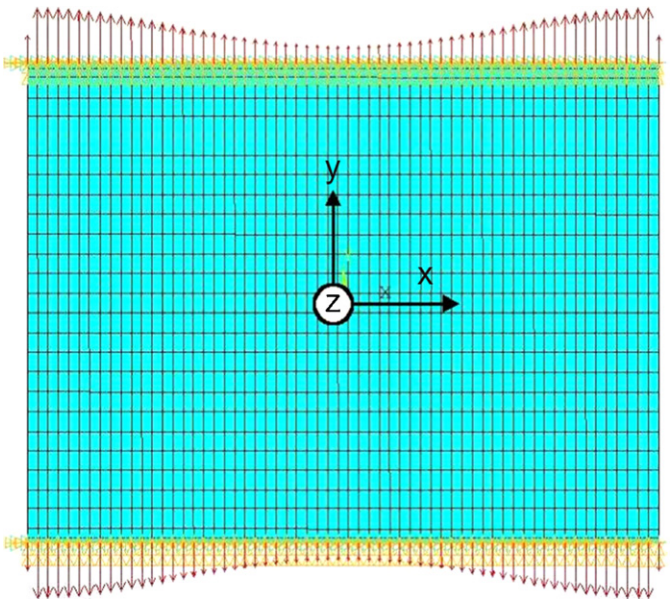

Fig. 1. FE model of a shadow-mask with a tension gradient.

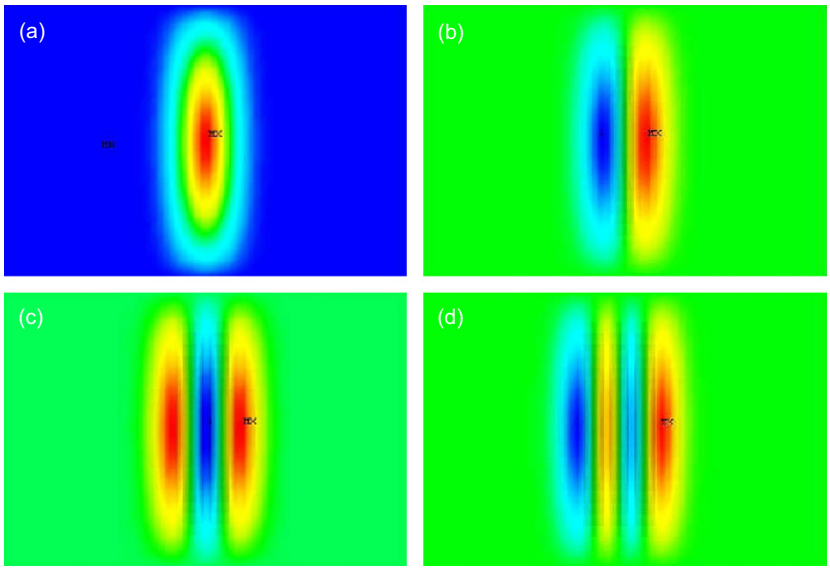

Fig. 2. Vibration mode shapes and natural frequencies of the shadow-mask: (a) first mode (183 Hz), (b) second mode (192 Hz), (c) third mode (201 Hz), and (d) fourth mode (209 Hz).

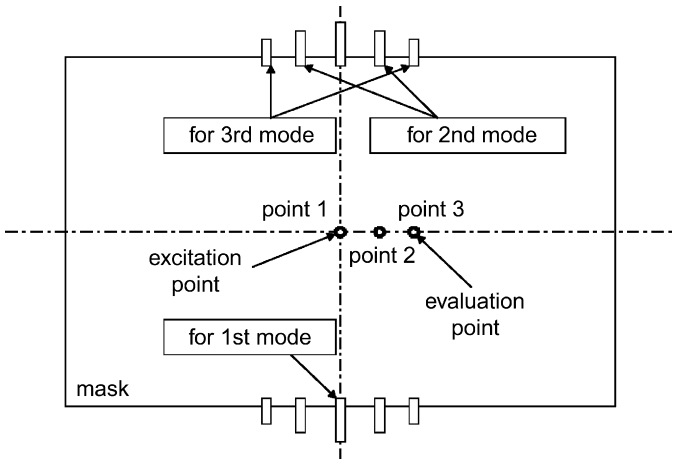

Fig. 3. Schematic diagram of the MDA mounted on the shadow-mask.

MDA, which consists of three different dynamic absorbers attached on the edge of shadow. The dynamic absorbers are arranged symmetrically from the centerline of the shadow-mask, and the number of absorbers depends on the number of objective vibration modes and the range to be controlled. In consideration of practical applications, the dynamic absorber is designed using a thin-plate cantilever and mounted on the edge of the shadow-mask where the electronic beam does not pass through the mask. The primary design parameters of the dynamic absorber, i.e., the mass, damping ratio, and tuning frequency, are determined by applying the design method of a simple dynamic absorber that can be used to control the vibration of a single-degree-of-freedom system. When applying this method to designing the cantilever, only the first bending mode is considered. A sensitivity analysis of the parameters using a FE model of the shadow-mask, subject to damping provided by the MDA, is performed in order to determine the design criteria.

3.1. Determination of the mass and its mass ratio

When designing the simple dynamic absorber, 10% of the mass of an objective system is generally recommended as the mass of the dynamic absorber [12]. However, it is difficult to follow this rule in designing the MDA for a system that has multiple vibration modes, because the mass obtained by this rule is so large that it generates mutual interference between the vibration modes. The masses of the MDA that yield two divided peaks which are nearly equally spaced on the frequency axis without modal interference are selected as the final design values. The masses of the cantilevers are determined for three objective modes of the shadow-mask, i.e., 1.48 g for the first mode, 0.82 g for the second mode, and 0.97 g for the third mode. The equivalent masses then are 0.341, 0.189, and 0.224 g based on Eq. (2) [13] at the end of a cantilever that has a first bending mode of vibration

$$m_{\mathrm{eq}} = 0.23m, \tag{2}$$

where m_{eq} is an equivalent mass and m is the mass of the cantilever. In order to determine the mass ratio for each mode, the modal equivalent mass of the shadow-mask should be calculated. The modal equivalent mass can be obtained by using the Rayleigh method [11] as follows:

$$M_{\mathrm{eq}_i} = \frac{2\mathrm{KE}_i}{v_{P_i}^2}, \tag{3}$$

where KE_i is the modal kinetic energy and v_{P_i} is the velocity at point P_i where the dynamic absorber corresponding to the ith mode is mounted. The MDA, as shown in Fig. 3, consists of 10 dynamic absorbers: two for the first mode, four for the second mode, and four for the third mode. The modal kinetic energies, velocities, and equivalent masses of three objective modes are summarized in Table 1. From the results, it can be observed that the mass ratios of the dynamic absorbers of the main system are only within 0.08%. These ratios are very small compared to the recommended mass ratio of 10%. In the sensitivity analysis, four different cases—half (case 1), one (case 2), two (case 3) and four (case 4) times the selected masses of the MDA—are tested. The damping ratio and tuning frequency, which are addressed in detail in the following sections, are calculated using the selected mass. Fig. 4 shows the receptances $\alpha_{11}(\omega)$ of four cases at the center point of the shadow-mask where the first vibration mode is most dominant. Two new resonant peaks appear at each side of the first mode of 183 Hz due to the dynamic absorber, i.e. splitting of the original resonance. As the mass of the dynamic absorber increases, the two resonant peaks become increasingly separated from each other and generates interference with the neighboring mode of 192 Hz. Fig. 5 shows the maximum displacements of the shadow-mask at three estimation points versus the MDA masses obtained from a sine swept test that a unit force is applied at the center point. The results illustrate that the selected MDA masses are sufficient to effectively reduce vibration.

3.2. Determination of the damping ratio

The optimal damping ratios (ζ_{opt}) of the MDA are calculated by substituting the mass ratio ($\mu = m/M_{\mathrm{eq}i}$) into Eq. (4) [13] as follows:

$$\zeta_{\mathrm{opt}} = \sqrt{\frac{3\mu}{8(1+\mu)^3}}. \tag{4}$$

Table 1
Modal kinetic energies, velocities, and equivalent masses at the position where the corresponding dynamic absorber is mounted

Mode	KE_i (J)	v_{P_i} (mm/s)	M_{eq_i} (g)
First	332	32.9	463
Second	185	28.4	311
Third	203	26.5	361

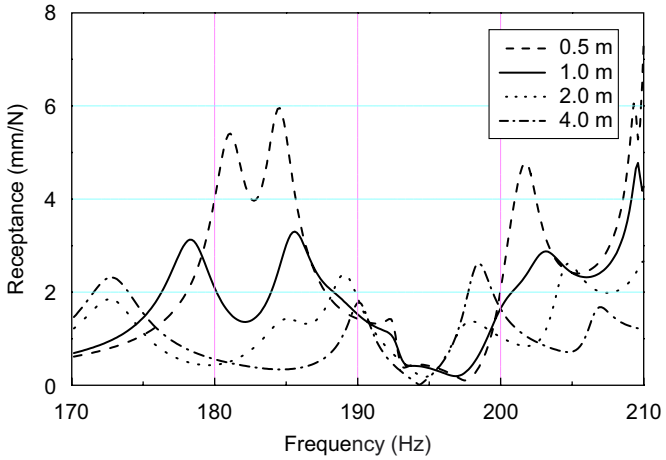

Fig. 4. Receptances, $\alpha_{11}(\omega)$ for different the MDA masses.

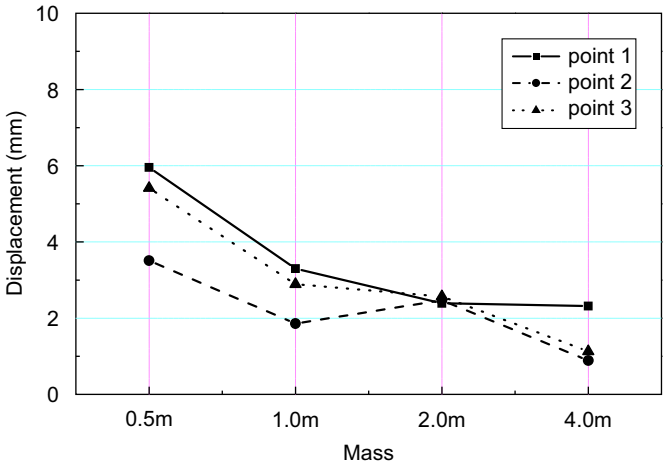

Fig. 5. Maximum displacements versus the MDA masses.

Table 2
Mass ratios, damping ratios, and tuning frequencies for different modes

Mode	Mass ratio (μ)	Damping ratio (ζ_{opt})	Tuning frequency (Hz)
First	7.36×10^{-4}	0.0166	182.89
Second	6.08×10^{-4}	0.0151	192.30
Third	6.19×10^{-4}	0.0152	201.06

From the mass ratios in Table 2 and Eq. (4), the optimal damping ratios are given as 1.5–1.7%, which is assumed to be a proportional damping in the response analysis. In the sensitivity analysis, four different cases—quarter (case 1), one (case 2), two (case 3) and four (case 4) times that of the optimal damping of the MDA—are tested. Fig. 6 shows the results of the receptances $\alpha_{11}(\omega)$ of these four cases. When the MDA has optimal damping, the two peak values divided from the original mode (183 Hz) become similar to each other. Fig. 7 shows the maximum displacements of the shadow-mask at three estimation points versus the damping ratios. These results show that the optimal damping cases are the most efficient in terms of reducing the vibration.

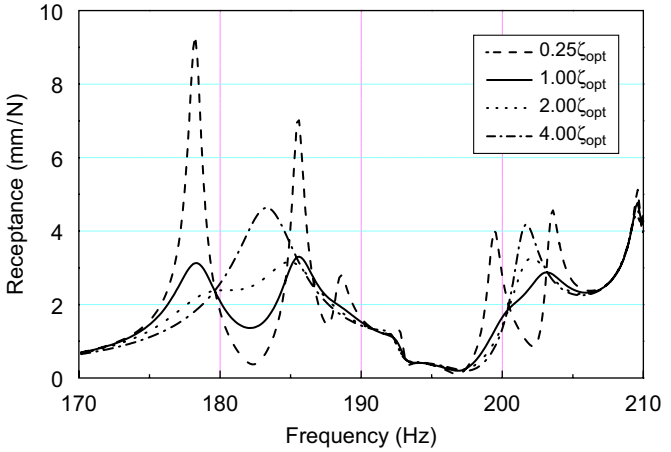

Fig. 6. Receptances, $\alpha_{11}(\omega)$ for different MDA damping ratios.

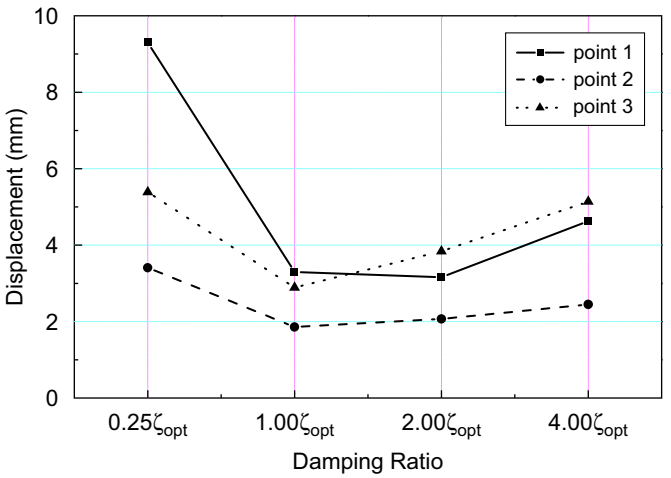

Fig. 7. Maximum displacements versus the MDA damping ratios.

3.3. Determination of the tuning frequency

The tuning frequency for each dynamic absorber is calculated after determining the masses and damping ratios of the MDAs, whose natural frequencies should finally be tuned in order to complete the MDA design. The tuning frequency ω_a is given as [13]

$$\omega_a = \frac{\omega_o}{1+\mu}, \tag{5}$$

where ω_o is the natural frequency of the main system. In this case, the tuning frequencies are very similar to the natural frequencies of the main system; $\omega_a \approx \omega_o$ because the mass ratios have very small values of less than 0.001. Since the MDA consists of thin-plate cantilevers, the tuning frequencies depend only on their dimensions—width (b), thickness (t), and length (l). For convenience, all dynamic absorbers are designed to have the same width of 10 mm. Since the design of the dynamic absorber is based on the first vibration mode of a cantilever, the natural frequency can be represented as follows [14]:

$$\omega_a = 1.875^2\sqrt{\frac{EI}{ml^3}}, \tag{6}$$

where m, l, I, and E represent the mass, length, moment of inertia for a cross-sectional area, and Young's modulus of the cantilever, respectively. The thickness (t) and length(l) of the cantilever, which satisfy the tuning frequency, may be determined by Eq. (6) and are given as

$$t = \sqrt[3]{\frac{m^2\omega_a}{\rho^2 b^2 c}}, \tag{7}$$

$$l = \sqrt[3]{\frac{cm}{\omega_a \rho b}}, \tag{8}$$

where $c = 1.1049\sqrt{E/\rho}$ is the wave speed, and ρ is the density of mass.

In the sensitivity analysis, the tuning frequency is tested with three cases: an exact frequency, and two frequencies with errors of ± 3 Hz. Fig. 8 shows the results of the receptances $\alpha_{11}(\omega)$ for different tuning frequencies. When the tuning frequencies include some errors, the two divided peak values of FRF become different from each other. Fig. 9 shows the maximum displacements at three estimation points versus the

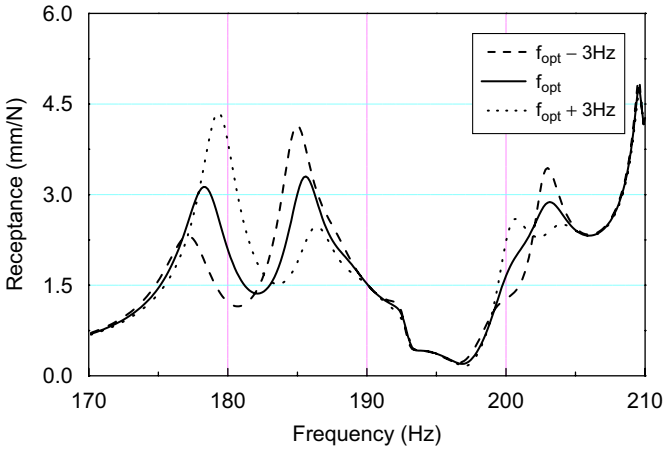

Fig. 8. Receptances, $\alpha_{11}(\omega)$ for different tuning frequencies.

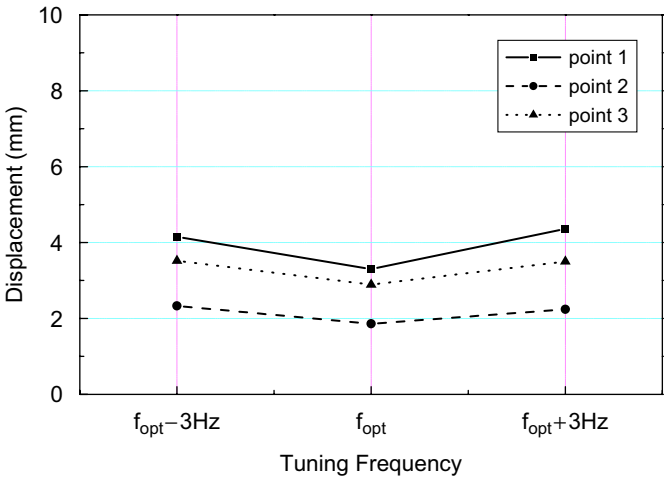

Fig. 9. Maximum displacements versus the MDA tuning frequencies.

tuning frequencies. The results illustrate that the case of exact tuning frequency has the best efficiency, but the sensitivity of the tuning frequency is relatively low compared to that of the mass and damping ratio.

3.4. Estimation of the MDA performance

A MDA targeting the reduction of three vibration modes of the shadow-mask is designed by the proposed method. The efficiency of the proposed MDA is then estimated through a response analysis of the FE model. The mass ratios, damping ratios, and tuning frequencies of the MDA obtained via the proposed method are summarized in Table 2. As previously mentioned, the mass ratios are very small values, below 0.1%, the damping ratios are 1.5–1.7%, and the tuning frequencies are similar to their corresponding natural frequencies. For comparison, the receptances, $\alpha_{11}(\omega)$, $\alpha_{21}(\omega)$, and $\alpha_{31}(\omega)$ for the shadow-mask with the MDA (solid line) and without a damping device (dashed line), are shown together in Fig. 10. As expected, the MDA successfully reduces the three objective modes of the shadow-mask.

4. Experiment and application

4.1. Design of the MDA

The proposed method is applied to the design of an MDA for a shadow-mask with a fundamental natural frequency of 131 Hz and 14 main vibration modes in the frequency band of 110–210 Hz, which is installed in a large size of CRT. General damping materials such as rubber or urethane cannot readily be applied to the MDA because the manufacturing environment of the CRT includes a high temperature process. The MDA is therefore made of thin-steel plates, which are bent in order to obtain impact damping from collision with the frame of the shadow-mask, as shown in Fig. 11. These thin plates maintain gaps in a size range of hundreds of micrometers between their end points and the frame so that they can easily collide. The damping ratio of impact is estimated as approximately 0.8% by the logarithmic decrement method. This value corresponds to half of the optimal damping ratio. Based on the analysis results, the average mass of the dynamic absorber, i.e., a thin-steel plate, is chosen as 1 g, which results in no interference between neighboring modes. The width and thickness of the dynamic absorber are determined as 10 and 0.25 mm, respectively, based on the mode shapes of the shadow-mask and the average mass. For convenience in manufacturing the MDA, a same width and thickness are applied to all dynamic absorbers. If the width and thickness of the dynamic absorber are given, the mass and tuning frequency can be determined simultaneously by modifying only the absorber's length. Through the determination process of the mass and tuning frequency of each dynamic absorber, the MDA, which consists of 14 dynamic absorbers, is finally designed as shown in Fig. 12. Consequently, since the shadow-mask is symmetric in the horizontal and vertical directions, four identical MDAs are finally mounted on the edge of the shadow-mask.

4.2. Experiments and discussion

An experiment is performed in a vacuum chamber based on consideration of the internal condition of the CRT, as shown in Fig. 13. A speaker attached at the front of a glass panel excites the shadow-mask and a laser sensor probes the velocity of the shadow-mask from the exterior through the window of the vacuum chamber. The speaker sweeps the natural frequency range of the shadow-mask with a sine signal of a function generator. Three variations of the shadow-mask (with damping wires, with MDAs, and without a damping device) are examined in order to evaluate the efficiency of the MDAs. Fig. 14 shows the estimated peaks of the velocity spectrums at the 14 points. The results show that the MDAs successfully reduce more than 60% of the vibration of the shadow-mask. It is also shown that the MDAs are more effective and stable than the damping wires in terms of reducing vibration at most points.

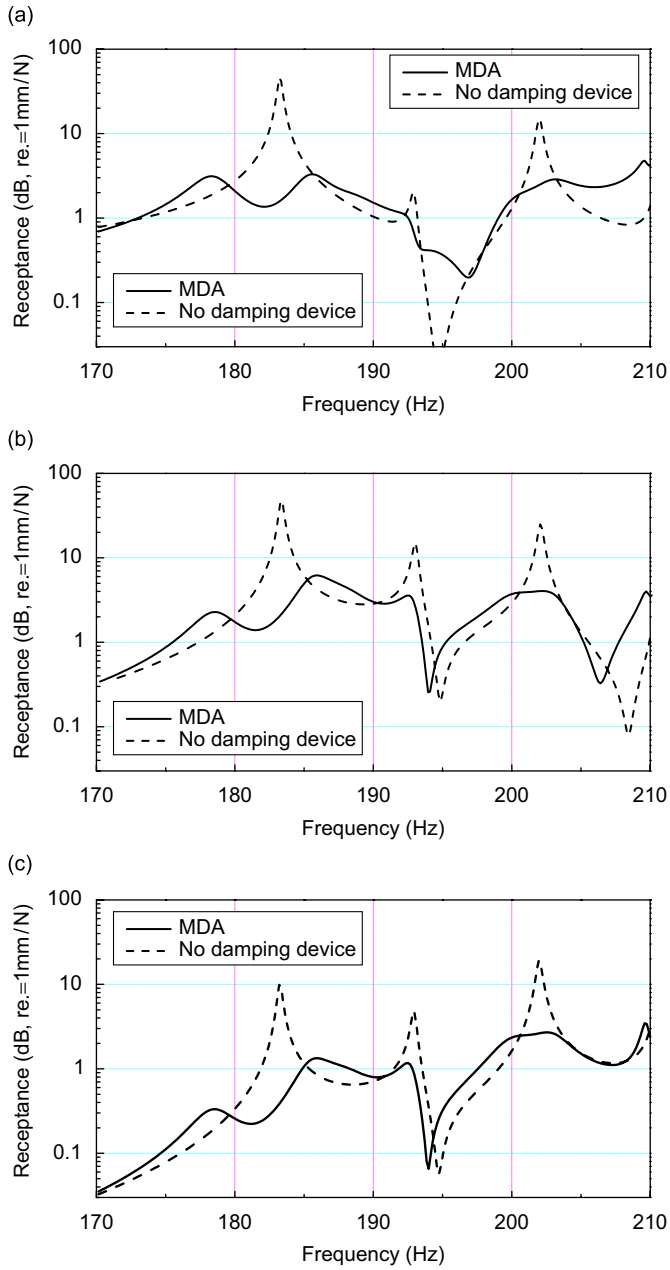

Fig. 10. Comparison of the receptances of shadow-masks with the MDA and without a damping device: (a) receptance $\alpha_{11}(\omega)$; (b) receptance $\alpha_{21}(\omega)$; and (c) receptance $\alpha_{31}(\omega)$.

5. Conclusion

An MDA consisting of several dynamic absorbers for reducing the vibration of a CRT shadow-mask was proposed. A design method for a MDA having a plate-type cantilever was proposed on the basis of sensitivity analysis of the FE model. The performance of the MDA designed by the proposed method was also verified by experiments. The FE model of the shadow-mask including the MDA was tested in order to derive the optimal values of the design parameters, i.e., the mass, damping ratio, and tuning frequency. It was found that the designed MDA effectively reduces the primary vibration modes of the

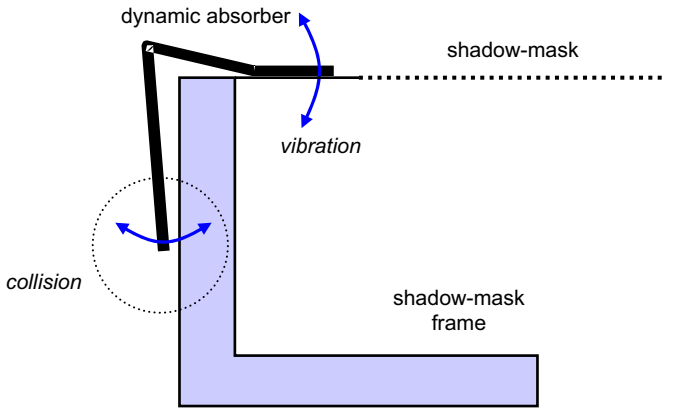

Fig. 11. Schematic diagram of the dynamic absorber with impact damping.

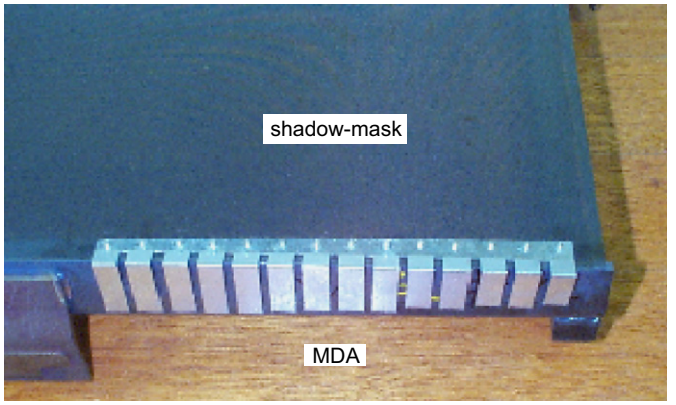

Fig. 12. MDA mounted on the shadow-mask.

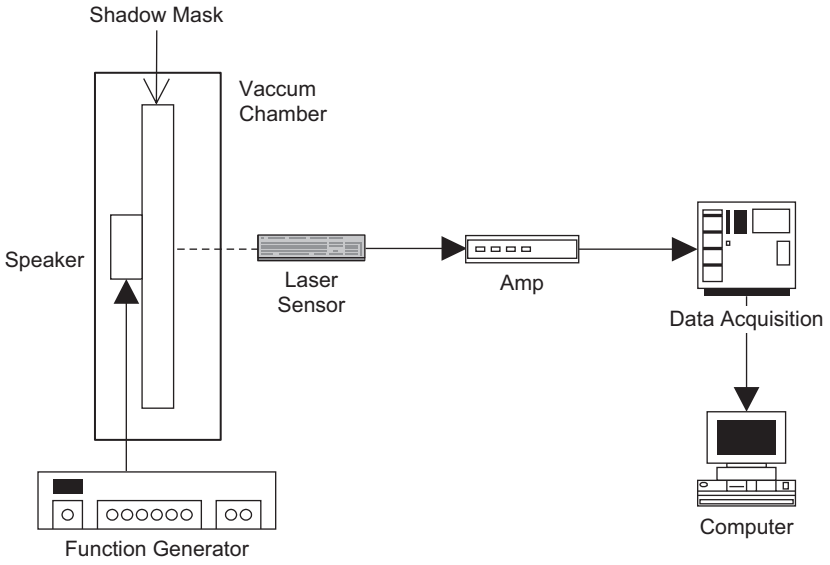

Fig. 13. Experimental setup.

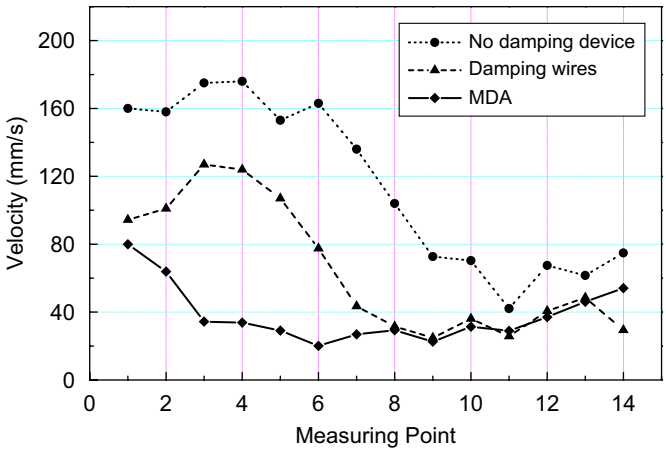

Fig. 14. Comparison of the maximum vibrations of shadow-masks with damping wires, with the proposed MDA, and without a damping device.

shadow-mask. The proposed MDA provides a new damping device that can replace damping wires and simultaneously avoid their drawbacks such as construction difficulty and the appearance of shadow lines on the screen.

Acknowledgment

The present research has been conducted by the Bisa Research Grant of Keimyung University in 2005.

References

[1] Shadow-mask for CRT, Japanese Patent 10-308182.
[2] Y. Ohmura, M. Hashimoto, H. Taguchi, Effect of damping wire on aperture grille vibration, *Proceedings of the IDW '99*, pp. 481–484.
[3] Shadow-mask for CRT, Japanese Patent 10-302665.
[4] Shadow-mask for CRT, Japanese Patent 10-172449.
[5] J. Ormondroyd, J.P. Den Hartog, The theory of the dynamic vibration absorber, *Transactions of the ASME* 50 (1928) 9–22.
[6] A.V. Srinivasan, Analysis of parallel damped dynamic vibration absorbers, *Journal of Engineering for Industry, Transactions of the ASME* 96 (1969) 2013.
[7] K. Seto, K. Iwanami, An investigation of the vibration isolator equipped dual dynamic dampers as a damping element, *Bulletin of the JSME* 24 (194) (1981) 2013.
[8] K. Seto, S. Yamashita, M. Okuma, A. Nagamatsu, Simultaneous optimum design method for multiple dynamic absorbers to control multiple resonance peaks, SAE No. 911067, pp. 229–237.
[9] S.C. Baek, 1995. Texture of Invar Sheet and Analysis of Perforated Sheet for Shadow-mask, PhD Thesis, Seoul National University.
[10] S.D. Kim, W.J. Kim, C.W. Lee, Vibration analysis of the tension shadow mask with wire impact damping, *Journal of Sound and Vibration* 265 (2003) 1003–1023.
[11] W.T. Thomson, *Theory of Vibration with Applications*, Prentice-Hall, Englewood Cliffs, NJ, 1993.
[12] J.P. Den Hartog, *Mechanical Vibrations*, Dover Publications, Inc., New York, 1984.
[13] C.M. Harris, *Shock and Vibration Handbook*, fourth ed., McGraw-Hill, New York, 1961.
[14] L. Meirovitch, *Principles and Techniques of Vibrations*, Prentice-Hall, Englewood Cliffs, NJ, 1997.